

Triggering Receptor Expressed on Myeloid Cells 2 (TREM2) R47H Variant Causes Distinct Age- and Sex-Dependent Musculoskeletal Alterations in Mice

Alyson L. Essex,^{1,2,3} Joshua R. Huot,^{3,4} Padmini Deosthale,^{1,2} Alison Wagner,¹ Jorge Figueras,¹ Azaria Davis,¹ John Damrath,⁵ Fabrizio Pin,^{3,4,6} Joseph Wallace,^{2,3,7} Andrea Bonetto,^{1,3,4,6} and Lilian I. Plotkin^{1,2,3}

¹Department of Anatomy, Cell Biology & Physiology, Indiana University School of Medicine, Indianapolis, IN, USA

²Roudebush Veterans Administration Medical Center, Indianapolis, IN, USA

³Indiana Center for Musculoskeletal Health, Indianapolis, IN, USA

⁴Department of Surgery, Indiana University School of Medicine, Indianapolis, IN, USA

⁵Weldon School of Biomedical Engineering, Purdue University, West Lafayette, IN, USA

⁶Simon Comprehensive Cancer Center, Indiana University, Indianapolis, IN, USA

⁷Department of Biomechanical Engineering, Indiana University-Purdue University Indianapolis, Indianapolis, IN, USA

ABSTRACT

Previous studies proposed the Triggering Receptor Expressed on Myeloid Cells 2 (TREM2), a receptor expressed in myeloid cells including microglia in brain and osteoclasts in bone, as a link between brain and bone disease. The TREM2 R47H variant is a known risk factor for Alzheimer's disease (AD), the most common form of dementia. To investigate whether altered TREM2 signaling could contribute to bone and skeletal muscle loss, independently of central nervous system defects, we used mice globally hemizygous for the TREM2 R47H variant (TREM2^{R47H/+}), which do not exhibit AD pathology, and wild-type (WT) littermate control mice. Dxa/Piximus showed bone loss in female TREM2^{R47H/+} animals between 4 and 13 months of age and reduced cancellous and cortical bone (measured by micro-computed tomography [μ CT]) at 13 months, which stalled out by 20 months of age. In addition, they exhibited decreased femoral biomechanical properties measured by three-point bending at 13 months of age, but not at 4 or 20 months. Male TREM2^{R47H/+} animals had decreased trabecular bone geometry but increased ultimate strain and failure force at 20 months of age versus WT. Only male TREM2^{R47H/+} osteoclasts differentiated more ex vivo after 7 days with receptor activator of nuclear factor κ B ligand (RANKL)/macrophage colony-stimulating factor (M-CSF) compared to WT littermates. Yet, estrogen receptor alpha expression was higher in female and male TREM2^{R47H/+} osteoclasts compared to WT mice. However, female TREM2^{R47H/+} osteoclasts expressed less complement 3 (C3), an estrogen responsive element, and increased protein kinase B (Akt) activity, suggesting altered estrogen signaling in TREM2^{R47H/+} cells. Despite lower bone volume/strength in TREM2^{R47H/+} mice, skeletal muscle function measured by plantar flexion and muscle contractility was increased in 13-month-old female mutant mice. Overall, these data demonstrate that an AD-associated TREM2 variant can alter bone and skeletal muscle strength in a sex-dimorphic manner independent of central neuropathology, potentially mediated through changes in osteoclastic intracellular signaling. © 2022 The Authors. *Journal of Bone and Mineral Research* published by Wiley Periodicals LLC on behalf of American Society for Bone and Mineral Research (ASBMR).

KEY WORDS: ALZHEIMER'S DISEASE; TREM2; MUSCLE; BONE FRAGILITY; OSTEOCLAST

Introduction

The economic and medical burden of age-related diseases continues to grow, and musculoskeletal disease including fractures continue to be among the most prevalent and costly

age-related complications, highlighting the importance of identifying effective interventions to improve musculoskeletal strength and function.⁽¹⁻³⁾ One of the most widespread age-related diseases is dementia, which is associated with lack of independence and increased death. Dementia is a broad term

This is an open access article under the terms of the [Creative Commons Attribution-NonCommercial-NoDerivs](https://creativecommons.org/licenses/by-nc-nd/4.0/) License, which permits use and distribution in any medium, provided the original work is properly cited, the use is non-commercial and no modifications or adaptations are made.

Received in original form December 3, 2021; revised form April 25, 2022; accepted May 11, 2022.

Address correspondence to: Lilian I. Plotkin, PhD, or Andrea Bonetto, PhD, Department of Anatomy, Cell Biology & Physiology, or Department of Surgery, Indiana University School of Medicine, Indianapolis, IN 46202, USA. E-mail: lplotkin@iu.edu (Plotkin); abonetto@iu.edu (Bonetto)

Additional Supporting Information may be found in the online version of this article.

Journal of Bone and Mineral Research, Vol. 37, No. 7, July 2022, pp 1366–1381.

DOI: 10.1002/jbmr.4572

© 2022 The Authors. *Journal of Bone and Mineral Research* published by Wiley Periodicals LLC on behalf of American Society for Bone and Mineral Research (ASBMR).

used to describe neurodegenerative diseases that cause declines in cognitive functions such as memory, the most prevalent being Alzheimer's disease (AD). AD is a neurodegenerative disease with distinct pathology including neuroinflammation, accumulation of amyloid- β (A β) plaques, and tau neurofibrillary tangles.⁽⁴⁾ Although AD is a disease of the brain, clinical evidence suggests that other tissues may be negatively impacted by AD, including bone and skeletal muscle. Clinical studies have demonstrated a significant association with cognitive decline, bone loss, and fracture risk,⁽⁵⁾ and a significant correlation between low bone mineral density (BMD) and lower brain volume, suggesting that AD may increase the risk for developing bone weakness.⁽⁶⁾ Further, retrospective studies have demonstrated that both low BMD and osteoporosis diagnosis were significant predictors of progression from mild cognitive impairment to diagnosed dementia, suggesting that bone loss may precede some of the clinical manifestations of AD.^(7,8) Skeletal muscle has also been shown to be negatively impacted by AD, based on evidence that female and male patients progressively lose skeletal muscle mass and strength as disease progression worsens compared to age and sex-matched controls, suggesting that AD may be exacerbating age-related loss of strength.^(9,10) However, whether bone and muscle loss are a direct result of the neurodegeneration or occurs due to a shared mechanism active in both brain and musculoskeletal tissues remains unknown.

Previous work in the amyloid precursor protein (APP) Swedish mutation (APP^{swe}) mouse model of AD has shown bone loss in the distal femur measured by micro-computed tomography (μ CT) in young but not in an aged mouse model of plaque neuropathology, as well as increases in osteoclast differentiation of cells from young but not old mice that cannot be singularly explained by the presence of A β .⁽¹¹⁾ Further work has demonstrated age-dependent loss of femoral bone mass in an amyloid precursor protein/presenilin 1 (APP/PS1) mouse model of plaque neuropathology, although in this mouse model the plaque density begins within 4 to 6 weeks postpartum and peaks around 8 months of age, whereas bone loss was only noted at 12 months.^(12,13) However, these data are limited and suggest that there may be mechanisms of AD-related bone loss that are not only independent of the central neuropathology but may be a consequence of age. To date, no mechanistic links between bone loss and AD have been identified, and the interaction between age and AD-related bone loss has never been explored. AD patients are more susceptible to falls and fractures, which often result from reduced skeletal muscle and bone strength.^(14,15) Therefore, understanding the mechanisms underlying bone and muscle loss in AD will be critical for finding therapeutic targets that could effectively reduce falls and fractures by targeting both tissues. Further, defining a potential mechanism of bone and muscle loss independent of central neurodegeneration will improve the overall understanding of neurodegenerative effects on peripheral physiology.

Triggering receptor expressed on myeloid cells 2 (TREM2) is a phagocytic receptor expressed on cells of the myeloid lineage including microglia, macrophages, and osteoclasts.⁽¹⁶⁾ TREM2 is used by microglia for synaptic pruning and in macrophages to aid in phagocytosis and inflammatory response.⁽¹⁷⁻¹⁹⁾ Additionally, TREM2 has been shown to contribute to the neuroinflammation that occurs during AD by altering microglial function.⁽²⁰⁻²²⁾ TREM2 has been shown to play a critical role in microglial response to AD pathology, being a receptor for the A β oligomers and dictating microglial response to plaque although not

triggering phagocytosis of the plaque but forming a barrier to prevent further expansion of the plaque.^(16,23,24) Previous studies on TREM2 signaling in murine osteoclasts have identified β -catenin as being a critical downstream mediator of TREM2 signaling in these cells, and TREM2 is known to contribute to osteoclast differentiation and resorption.^(25,26) Although the role of wild-type TREM2 in osteoclasts is somewhat understood, whether TREM2 may also contribute to AD-related degeneration beyond the brain such as bone fragility remains unexplored. Previous work by Jay and colleagues^(16,27) have primarily used TREM2 knockout models that do not express any TREM2 receptor to understand TREM2 signaling and consequences. However, knockout models may not explain how amino acid mutations that alter TREM2 signaling contribute to the observed increased risk for AD.

Genomewide associations studies (GWAS) have identified the R47H variant of the TREM2 gene to significantly increase the risk for developing AD.⁽²⁸⁾ The TREM2 R47H variant has previously been shown to have a phenotype in brain similar to that of a heterozygous knockout in a mouse model of AD, decreasing microglial response to plaque by reducing the plaque-barrier function of microglia.⁽²⁹⁾ However, the TREM2 R47H variant has also been shown to alter intracellular signaling, specifically phospho-Syk, without having an observable phenotype on macrophages differentiated from human induced-pluripotent stem cell macrophages.⁽³⁰⁾ Biochemical work has demonstrated that the R47H mutation occurs in the ligand binding domain of the receptor, and these effects of the R47H mutation in microglia and macrophages are likely due to changes in receptor binding to ligand.⁽³¹⁾ Previous work in Nasu-Hakola neurodegenerative disease has identified variants in TREM2 that impact bone and brain simultaneously.⁽³²⁾ However, no such work has identified a similar effect of TREM2 variants on brain and bone that are associated with AD. Further, it remains unclear whether AD-associated bone loss is secondary to the neurodegeneration or if mechanisms of bone loss occur independent of the neurodegeneration.

Therefore, we assessed whether a genetic variant in TREM2 known to contribute to high risk of developing AD could also be involved in bone loss independent of central neurodegeneration pathology. To do this, we utilized global TREM2^{R47H/+} mice and WT littermates to evaluate whether the AD-associated R47H variant in TREM2, identified in GWASs to increase risk for developing AD by threefold to fourfold, could also contribute to the bone and muscle weakness seen clinically.^(28,33) These mice have no additional mutations that would be needed to cause AD pathology, and thorough characterization of mice homozygous for the R47H mutation has shown that mice with this mutation do not develop AD pathology.^(34,35) These results are the first to define a potential mechanism of AD-associated bone loss independent of neurodegeneration and suggest that TREM2 may be a common link between AD-related degeneration of brain and bone. Further, these data are the first to demonstrate a potential role for TREM2 in loss of skeletal muscle strength and aging.

Materials and Methods

Mice

TREM2^{R47H/+} mutant mice were generated by The Jackson Laboratory (Bar Harbor, ME, USA) in collaboration with the Model-AD center (<https://www.model-ad.org/>) using clustered regularly

interspaced short palindromic repeats (CRISPR)/CRISPR-associated protein 9 (CRISPR/Cas9) genome editing as described.⁽²⁹⁾ Animals were maintained heterozygous for the global TREM2 R47H mutation (TREM2^{R47H/+}) and wild-type TREM2^{+/+} (WT) littermates were used as controls. Single-nucleotide polymorphism (SNP)-based genotyping (Thermo Fisher Scientific, Waltham, MA, USA) was used to identify carriers in subsequent crosses using the following: forward primer: 5'-ATGTACTTATGACGCCTGAAGCA, reverse primer: 5'-ACCCAGCTGCCGACAC, SNP reporter 1: 5'-CCTTGGCTCTCCC, SNP reporter 2: 5'-CCTTGTGTCTCCC. All mice presented C57BL/6J background, were fed a regular diet and water ad libitum, and maintained on a 12-hour light/dark cycle. All animal studies were approved by the Institutional Animal Care and Use Committee of Indiana University School of Medicine.

Quantitative PCR

Total RNA from ex vivo isolated and differentiated osteoclasts, whole tibias, whole brain, and gastrocnemius muscles was isolated using TRIzol (Invitrogen, Grand Island, NY, USA).⁽³⁶⁾ Reverse transcription was performed using a high-capacity cDNA kit (Applied Biosystems, Foster City, CA, USA). Quantitative PCR (qPCR) was performed using the Gene Expression Assay Mix TaqMan Universal Master Mix with the 7500 Real Time PCR/StepOne Plus system and software (Life Technologies, Inc., Grand Island, NY, USA). Gene expression was corrected by the levels of the housekeeping gene glyceraldehyde 3-phosphate dehydrogenase (GAPDH). Primers and probes were commercially available (Applied Biosystems) or were designed using the Assay Design Center (Roche Applied Science, Indianapolis, IN, USA). Relative expression was calculated using the delta threshold cycle (Δ Ct) method.

Body weight and BMD

BMD was measured regularly from 1 to 20 months of age by DXA/PIXImus (GE Medical Systems, Lunar Division, Madison, WI, USA).⁽³⁶⁾ Body weight was measured at the time of the DXA scan. BMD measurements included total (whole body excluding the head and tail), femur, and spine (L₁–L₆). Calibration was performed using a standard control phantom before scanning, as recommended by the manufacturer.

Body composition assessment

Lean (muscle) and fat (adipose) mass was assessed at baseline and the day before sacrifice in physically restrained mice, by means of an EchoMRI-100 (EchoMRI, Houston, TX, USA), as published.⁽³⁷⁾

μ CT analysis of femurs bone morphometry

μ CT scanning was performed to measure morphological and bone mass indices of femoral bone.^(38,39) After euthanasia, the left femurs were wrapped in saline-soaked gauze and frozen at -20°C until imaging. Bone samples were rotated around their long axes and images were acquired using a Bruker Skyscan 1176 (Bruker, Kontich, Belgium) with the following parameters: pixel size = $9\mu\text{m}^3$; peak tube potential = 65 kV; X-ray intensity = $300\mu\text{A}$; 0.7-degree rotation step. Calibration of the grayscale levels was performed using hydroxyapatite (HA) phantoms (0.25 and 0.75g/cm^3 Ca-HA). Based on this calibration and the corresponding standard curve generated, the equivalent minimum calcium hydroxyapatite level was 0.42

g/cm^3 . Raw images were reconstructed using the SkyScan reconstruction software (NRecon; Bruker) to three-dimensional (3D) cross-sectional image data sets using a 3D cone beam algorithm. Structural indices of the trabecular bone were calculated on reconstructed images using the Skyscan CT Analyzer software (CTAn; Bruker). Cortical bone was analyzed by threshold of 80–255 in a 100-slice selection of the femoral mid-shaft using code as described.⁽³⁸⁾ Cortical bone parameters included periosteal bone surface (Ps.BS), endocortical bone surface (Ec.BS), bone area/ total area (BA/TA or Ct.Ar/Tt.Ar), cross-sectional tissue (bone + bone marrow) area (Tt.Ar or Total cross-sectional area [CSA]), marrow area, cortical bone area (Ct.Ar), cortical thickness (Ct.Th), and moment of inertia. Trabecular bone was analyzed between 0.5 and 1.0 mm above the femoral distal growth plate using a threshold of 80–255 at 4 and 13 months and 50–255 at 20 months. Trabecular parameters included bone volume fraction (BV/TV), number (Tb.N), thickness (Tb.Th), and separation (Tb.Sp).

Three-point bending

Following μ CT, left femurs were thawed and mechanically tested using a three-point monotonic test to failure.⁽³⁸⁾ Femurs were loaded with the anterior surface in tension at a rate of 0.025 mm/s and a lower support span of 8 mm. Sample hydration was maintained with phosphate-buffered saline (PBS) throughout testing. The values of c-anterior extreme fiber length, the furthest distance from the bone centroid to the surface in tension, and I_{ML} , the moment of inertia about the medial-lateral axis, obtained from μ CT of the mid-diaphysis were then used to normalize force-displacement data into stress-strain data and calculate estimated material level properties,⁽⁴⁰⁾ using standard beam bending equations, as described.⁽³⁸⁾

Bone histomorphometry

Femurs harvested from 13-month-old female mice were fixed in 10% neutral buffered formalin, cut, and embedded in plastic and paraffin using previously established methods at the Indiana Center for Musculoskeletal Health Histology and Histomorphometry Core.⁽⁴¹⁾ To allow for dynamic histomorphometric analysis, mice were injected intraperitoneally with calcein (30 mg/kg; Sigma-Aldrich, St. Louis, MO, USA) and Alizarin red (50 mg/kg; Sigma-Aldrich) 7 and 2 days prior to euthanasia. Dynamic histomorphometry was performed on unstained, undemineralized methyl methacrylate-embedded distal femur cross-sections using an epifluorescence microscope. Osteoclasts were quantified in demineralized, paraffin-embedded femoral bone mid-diaphysis cross-sections stained for tartrate-resistant acid phosphatase (TRAP)/Toluidine blue. Histomorphometric analyses were performed using OsteoMeasure high-resolution digital video system (OsteoMetrics Inc., Decatur, GA, USA). The terminology and units used are those recommended by the American Society for Bone and Mineral Research (ASBMR) Histomorphometry Nomenclature Committee.⁽⁴²⁾

Osteoclast assays

Bone marrow cells (BMCs) were isolated from 4-month-old female and male WT and TREM2^{R47H/+} C57BL/6J mice by flushing the bone marrow out with 10% fetal bovine serum (FBS)-containing and 1% penicillin/streptomycin (P/S)-containing α -modified essential medium (α -MEM) and cultured for 48 hours.^(36,43) Nonadherent cells were then collected and $2 \times$

10^4 cells/cm² were seeded on 96-well plates. Receptor activator of nuclear factor κ B ligand (RANKL) (80 ng/mL) and macrophage colony-stimulating factor (M-CSF) (20 ng/mL) were added to induce osteoclast differentiation and media was changed every 2 to 3 days for 2, 5, or 7 days. Cells were stained using a TRAPase kit (Sigma-Aldrich) and mature osteoclasts that stained TRAP-positive and exhibiting three or more nuclei were quantified. Parallel cultures were generated to generate RNA and protein lysates.

Multiplex cell-signaling assays

Kinase activation was measured in osteoclast protein lysates made from ex vivo bone marrow cells from WT and TREM2^{R47H/+} animals after 7 days of differentiation, as described in the Osteoclast assay section above, using the Bioplex protein array system at the Multiplex Analysis Core (MAC) at Indiana University School of Medicine (IUSM). Premixed magnetic beads of the Milliplex multi-pathway 9-plex phospho- and total protein kits were used (Milliplex, Burlington, MA, USA).

Grip strength measurement

Forelimb strength was assessed using a commercially available grip strength meter (Columbus Instruments, Columbus, OH, USA), as described.⁽⁴⁴⁾ The absolute force (expressed in grams) and the normalized force (expressed as grams of force/body weight) were recorded. To reduce procedure-related variability, the same operator analyzed an average from several repeated peak force measurements in the same animal in a blind manner. For this assay, five measurements were performed, and the top three measurements were used for the analysis. Moreover, to avoid bias of habituation, the animals were tested every month during development (1–4 months of age) and every 2 to 5 months as the animals aged.

In vivo muscle contractility

Female and male WT and TREM2^{R47H/+} mice at 12 months of age were tested for muscle force by in vivo plantarflexion 2 days prior to euthanasia (Aurora Scientific, Aurora, ON, Canada), as described.^(45,46) Briefly, the left hind foot was taped to the force transducer and positioned to where the foot and tibia were aligned at 90 degrees. The knee was then clamped at the femoral condyles, avoiding compression of the fibular nerve. Two disposable monopolar electrodes (Natus Neurology, Middleton, WI, USA) were placed subcutaneously posterior/medial to the knee in order to stimulate the tibial nerve. Peak twitch torque was first established in order to determine maximal stimulus intensity. Following determination of stimulus intensity, mice were subjected to an incremental frequency stimulation protocol to assess force–frequency relationships. The protocol utilized 0.2-ms pulses at 10, 25, 40, 60, 80, 100, 125, and 150 Hz with 1 minute in between stimulations.

In vivo electrophysiology

Triceps surae muscles of female and male WT and TREM2^{R47H/+} mice 12 months of age were subjected to electrophysiological functional assessment using the Sierra Summit 3-12 Channel EMG (Cadwell Laboratories Incorporated, Kennewick, WA, USA), as described.⁽⁴⁷⁾ Two 28G stimulating needle electrodes (Natus Neurology, Middleton, WI, USA) were used to stimulate the sciatic nerve of the left hindlimb, a duo shielded ring electrode

(Natus Neurology) was used for recording, and a ground electrode was placed over the animal's tail. Baseline-to-peak and peak-to-peak compound muscle action potential (CMAP) responses were recorded utilizing supramaximal stimulations (constant current intensity: <10 mA; pulse duration: 0.1 ms) as described.⁽⁴⁶⁻⁴⁸⁾

Ex vivo contractility

The whole muscle contractility of the extensor digitorum longus (EDL) and soleus muscles was determined as described.⁽⁴⁵⁾ EDL and soleus muscles were dissected from hind limbs, the tendons were tied to stainless steel hooks using 4-0 silk sutures, and the muscles were mounted between a force transducer (Aurora Scientific, Aurora, ON, Canada). The muscles were then immersed in a stimulation bath with O₂/CO₂ (95/5%) and Tyrode solution (121mM NaCl, 5.0mM KCl, 1.8mM CaCl₂, 0.5mM MgCl₂, 0.4mM NaH₂PO₄, 24mM NaHCO₃, 0.1mM ethylenediamine tetraacetic acid [EDTA], and 5.5mM glucose). The muscles were stimulated to contract using supramaximal stimuli between two platinum electrodes. Data were collected via the Dynamic Muscle Control/Data Acquisition (DMC) and Dynamic Muscle Control Data Analysis (DMA) programs (Aurora Scientific). Prior to each contraction bout, the muscle was lengthened to yield the maximum force (L0). The force–frequency relationships were determined via an incremental stimulation frequency protocol (0.5-ms pulses at 10, 25, 40, 60, 80, 100, 125, and 150 Hz for 350 ms (EDL) or 600 ms (Soleus) at the supramaximal voltage) with 1-minute rest periods between contractions. Following force frequency assessment, muscles rested for 5 minutes and then underwent a 60-contraction (EDL) or 100-contraction (Soleus) fatiguing protocol at 60 Hz (every 3 seconds). The muscle weight and L0 were used to determine the specific force.

Activity monitoring

Female and male WT and TREM2^{R47H/+} mice at 12 months of age were placed one at a time in an Opto-Varimex Auto Track System (Columbus Instruments, Columbus, OH, USA), where activity was tracked and categorized across 2 minutes.

C2C12 Myotube differentiation

Murine C2C12 skeletal myoblasts (ATCC, Manassas, VA, USA) were grown in high-glucose Dulbecco's modified Eagle medium (DMEM) supplemented with 10% FBS, 100 U/mL penicillin, 100 mg/mL streptomycin, 2mM L-glutamine, and maintained at 37°C in 5% CO₂, as published.⁽⁴⁹⁾ Myotubes were generated by exposing the myoblasts to DMEM containing 2% horse serum (ie, differentiation medium [DM]), and replacing the medium every other day for 3 days. In order to determine the dependence of myotube size on bone-derived factors, myotubes were exposed to 5% bone conditioned medium (CM) for 48 hours. Cells were fixed and stained as described.⁽³⁷⁾

Generation of bone-derived CM

Right femur and tibias from 4-month-old female and male WT and TREM2^{R47H/+} mice were carefully cleaned of muscle and fibrous tissues, epiphyses cut, and then marrow-flushed multiple times with α -MEM. These long-bone cortical preparations were then cultured ex vivo in 10% FBS and 1% P/S- α -MEM for 48 hours as described.⁽⁵⁰⁾ CM was collected and stored at –20°C prior to C2C12 exposure.

Assessment of myotube size

Cell layers were fixed in ice-cold acetone-methanol (50:50) and incubated with an anti-Myosin Heavy Chain antibody (MF20, 1:200; Developmental Studies Hybridoma Bank, Iowa City, IA, USA) and an AlexaFluor 488-labeled secondary antibody (Invitrogen, Grand Island, NY, USA) as described.⁽³⁷⁾ Analysis of myotube size was performed by measuring the average diameter of long, multinucleate fibers avoiding regions of clustered nuclei on a calibrated tissue image using the ImageJ 1.43 software (NIH, Bethesda, MD, USA; <https://imagej.nih.gov/ij/>).⁽⁵¹⁾

Statistics

All statistical analyses were performed using GraphPad Prism 9.0.0 (GraphPad Software, San Diego, CA, USA). In general, one-tailed or two-tailed Student's *t* tests were performed to determine significant differences between TREM2^{R47H/+} and WT groups for each sex; comparisons were not made between sexes as indicated in the figure legends.^(52,53) For data that failed either the D'Agostino and Pearson test or Shapiro-Wilk test for normality, analysis was performed using the Mann-Whitney test, and for data with unequal variance, the Welch's *t* test was used as indicated in the corresponding figure legends. For longitudinal data taken across 20 months, multiple frequencies, or contractions, a two-way analysis of variance (ANOVA) was performed, followed by post hoc comparisons for each time point. Post hoc tests used is specified in the figure legends and vary depending on the comparison being made. All results of the ANOVA tests are included in Table S1. Statistical significance was set at $p \leq 0.05$, and the data are presented as box plots where the horizontal line represents the median, the box outlines the interquartile range, and the bars represent maximum and minimum, whereas each dot corresponds to an individual animal. For longitudinal data, the symbol represents the median and bars represent the interquartile range. Sample sizes vary due to variability in genotypes generated as data was collected, and samples were excluded if damaged during collection or analysis (eg, femurs broken excluded from μ CT analysis).

Results

TREM2 R47H mutation does not alter bone through skeletal maturity

The TREM2 R47H variant has been shown to impact messenger RNA (mRNA) splicing of the TREM2 transcript in cortical brain and microglia lysates, producing a protein expression knock-down similar to that of a heterozygous knockout, evident by decreases in mRNA expression measured by qPCR of the TREM2 gene.^(29,54) However, qPCR analysis of both whole bone and ex vivo osteoclast cultures, comparable to cortical brain and microglia, respectively, from female and male WT and TREM2^{R47H/+} bone marrow cells demonstrates that expression of the TREM2 R47H variant does not result in a different splicing variant in these tissues (Fig. S1A). This evidence suggests that the TREM2 gene may be spliced differently in bone versus brain, and that the consequences of TREM2 R47H expression in bone are not due to reduced expression levels.

Ex vivo μ CT analyses showed no differences in trabecular (Fig. 1A) or cortical (Fig. 1B) bone geometry in male or female TREM2^{R47H/+} animals compared to WT littermates at 4 months of age. On the other hand, three-point bending analysis demonstrated that the pre-yield displacement was decreased in female

TREM2^{R47H/+} animals compared to WT littermates (Fig. 1C). These data demonstrate that by skeletal maturity, the TREM2 R47H variant has no effect on bone geometry and only a mild effect on mechanical integrity noted in the pre-yield displacement, and only in female animals. However, BMD gain between 1 and 12 months of age was significantly lower in the femur, but not spine or total BMD, in female TREM2^{R47H/+} mice, compared to WT littermates (Fig. S1B). On the other hand, no differences in BMD at each age or in bone gain were detected in males up to 20 months.

TREM2^{R47H/+} female mice have weaker, smaller bones at 13 months of age

Based on the differences in BMD accrual, we analyzed bone mass and strength in femoral bones of female WT and TREM2^{R47H/+} mice at 13 months of age. Thirteen-month-old TREM2^{R47H/+} female animals had decreased trabecular bone volume/total volume and, trabecular thickness, a larger trabecular separation, and a lower trabecular number in the distal femur compared to WT littermates (Fig. 2A). Additionally, TREM2^{R47H/+} female mice had significantly increased marrow area, lower cortical thickness and bone area/total area, an increased total cross-sectional area, and endocortical bone surface compared to WT littermates (Fig. 2B). These data demonstrate that the TREM2^{R47H/+} cortical bone is thinner but wider, suggesting the TREM2 R47H variant may accelerate age-related bone loss patterns of endosteal resorption sometime between 4 and 13 months of age. Ex vivo three-point bending analysis demonstrated that TREM2^{R47H/+} female femurs are weaker than WT, indicated by lower mechanical properties of the bone such as yield force, work to yield (Fig. 2C). Interestingly, TREM2^{R47H/+} female mice had an increased postyield displacement compared to WT, suggesting the bones are more ductile (Fig. 2B). Estimations of the material properties of the female TREM2^{R47H/+} femurs were also decreased compared to WT as exemplified in the representative stress-strain graph, including a decreased yield stress, resilience, ultimate stress, and modulus compared to WT littermate controls (Fig. 2C). These data suggest that the TREM2 R47H variant has a deleterious effect on bone geometry as well as bone mechanical and material properties in female animals at 13 months of age.

TREM2^{R47H/+} mice have less bone volume, but are not weaker, at 20 months of age

At 20 months of age, ex vivo μ CT analysis of TREM2^{R47H/+} animals did not show differences in cancellous bone volume of the distal femur of female compared to WT mice (Fig. 3A). However, analysis at the femoral mid-diaphysis shows that female TREM2^{R47H/+} mice have decreased cortical area and periosteal bone surface, as well as a smaller cross-sectional area compared to WT littermates (Fig. 3B). Female TREM2^{R47H/+} femurs have a decreased moment of inertia compared to WT littermates (Fig. 3B). The TREM2^{R47H/+} femurs also showed a trend toward decreased tissue mineral density (TMD) (Fig. 3C) of the cortical bone compared to WT littermates but have similar mechanical and estimated material properties of the femur at 20 months of age by three-point bending compared to WT mice (Fig. 3C). These data suggest that the bone deterioration present in 13-month-old TREM2^{R47H/+} female mice is not continually exacerbated through 20 months of age. Further, our evidence is consistent with an accelerated skeletal aging in TREM2^{R47H/+} females up to 13 months, a process that stalls out allowing for the aging

4 months of age

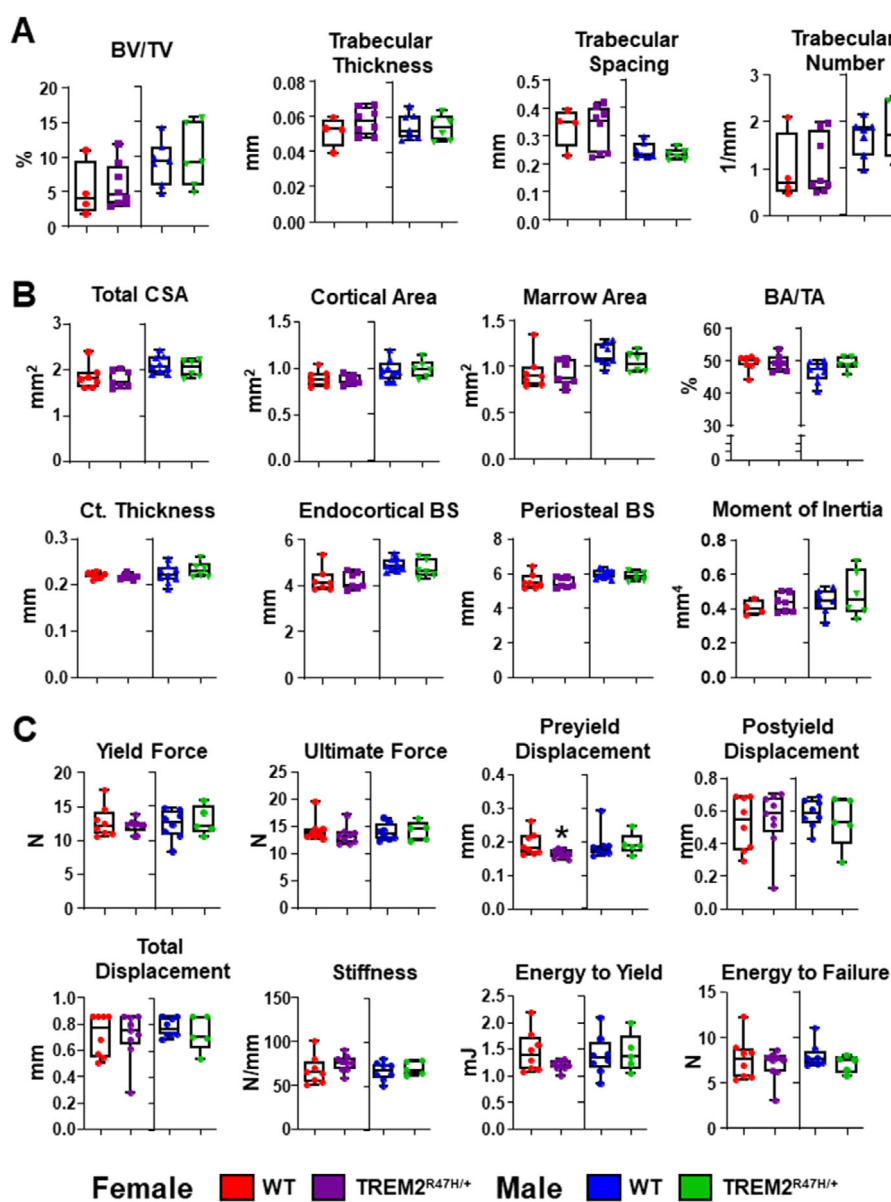


Fig. 1. TREM2^{R47H/+} has minimal effect on bone strength in female mice, but no effect on bone volume at 4 months of age. μ CT analysis of cancellous bone of the femoral mid-diaphysis ($n = 4-8$ /group) (A), cortical bone of the distal femur ($n = 6-9$ /group) (B), and (C) three-point bending mechanical testing ($n = 5-9$ /group) in 4-month-old male and female TREM2^{R47H/+} and WT mice. Comparisons are sex-matched between TREM2^{R47H/+} versus WT using Welch's t test: female pre-yield displacement $p = 0.042$, energy to yield $p = 0.072$.

WT mice to catch up, resulting in comparable bone mass and strength in TREM2^{R47H/+} and WT mice at 20 months of age.

Male TREM2^{R47H/+} animals did have decreases in cancellous bone, including decreased trabecular number, increased trabecular spacing, and a trend toward a decrease in the percent bone volume/total volume in the distal femur compared to WT littermates of the same age (Fig. 3A). However, even with the added impact of aging, male TREM2^{R47H/+} animals had no differences in the cortical bone geometry at the femoral mid-diaphysis compared to WT animals (Fig. 3B). Interestingly, three-point bending shows that male TREM2^{R47H/+} femurs have mild increases in the

ultimate strain and failure force mechanical properties, but no difference in tissue mineral density (TMD) or any other estimated strength properties (Fig. 3C). Together, these data indicate that male TREM2^{R47H/+} may be impacted by the TREM2 R47H variant, but only at an aged time point, whereas female animals are most strongly impacted at an intermediate aged time point (13 months). Further, there is a disparate effect of the variant in male mice at 20 months of age, with reduced cancellous bone mass and increased cortical bone strength. Overall, these data demonstrate that the TREM2 R47H variant has a sex- and age-dependent effect on both bone geometry and strength.

13 months of age

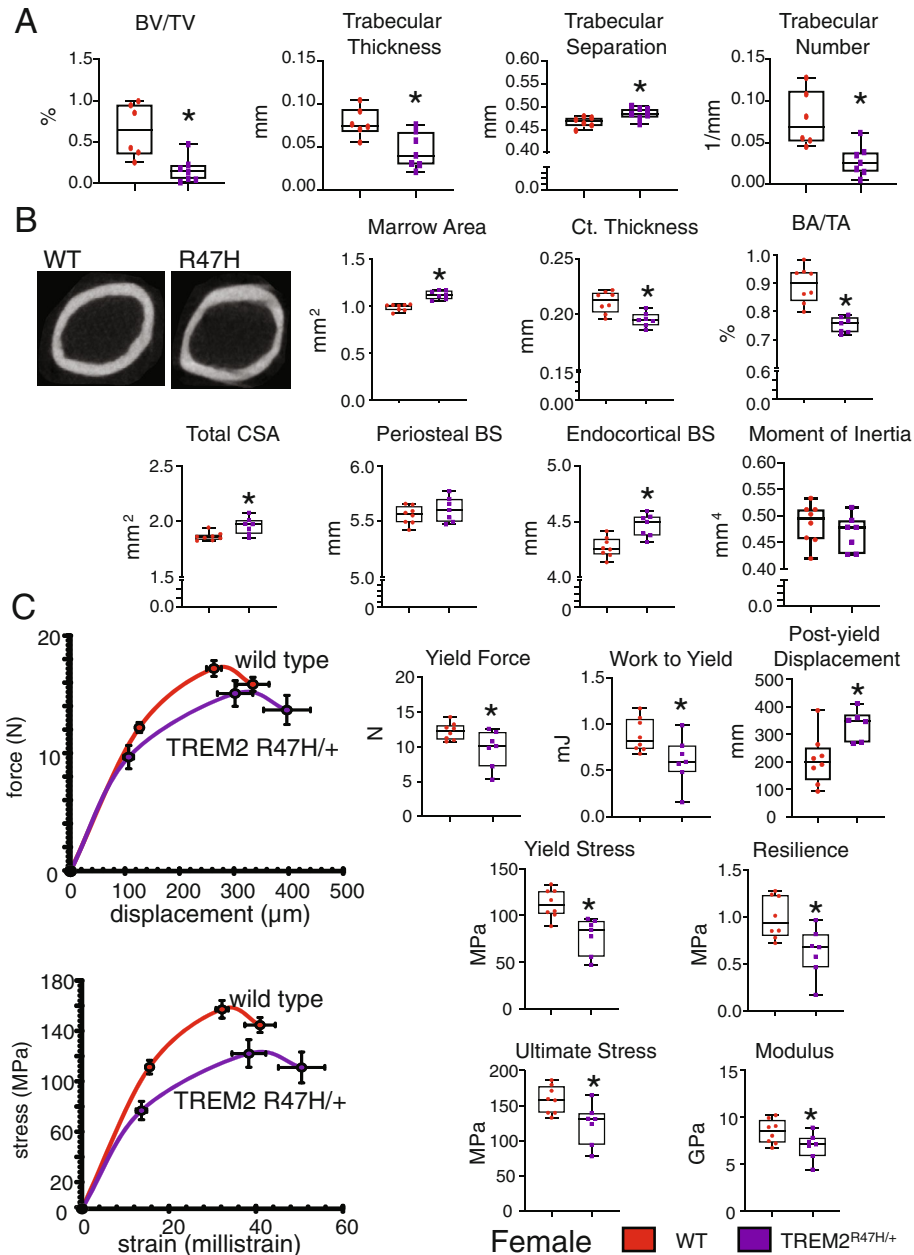


Fig. 2. Female TREM2^{R47H/+} mice have bone loss and mechanical weakness at 13 months of age. μ CT analysis of cancellous bone of the femoral mid-diaphysis ($n = 7-8$ /group) (A), cortical bone of the distal femur ($n = 7$ /group) (B), and three-point bending mechanical testing ($n = 7$ /group) (C) in 13-month-old female TREM2^{R47H/+} and WT mice. Representative images of female WT and TREM2^{R47H/+} cortical bone oriented with the medial-lateral angled on the x-axis are shown. Mechanical and material strength representative graphs have plotted the 0, yield, maximum load, and failure points. Comparisons between female TREM2^{R47H/+} versus WT using Student's *t* test: (A) Marrow area $p = 0.00002$, Ct. thickness $p = 0.003$, BA/TA $p = 0.00008$, Total CSA $p = 0.007$, Ec.BS $p = 0.0017$. (B) BV/TV $p = 0.0027$, Trabecular thickness $p = 0.009$, Trabecular separation $p = 0.015$, Trabecular number $p = 0.002$. (C) Yield force $p = 0.029$, Work to yield $p = 0.031$, Post-yield displacement $p = 0.011$, Yield stress $p = 0.0019$, Resilience $p = 0.01$, Ultimate stress $p = 0.015$, Modulus $p = .048$.

TREM2^{R47H/+} osteoclasts have sex-dependent changes in osteoclast function

Because TREM2 is primarily expressed on cells of the myeloid lineage, we investigated whether the TREM2 R47H variant

increased osteoclast differentiation similar to what has been previously reported in TREM2 null osteoclasts.⁽²⁶⁾ Although decreases in cortical and cancellous bone volume were found in 13-month-old female TREM2^{R47H/+} femurs compared to WT, there were no changes in osteoclast number, osteoclast surface,

20 months of age

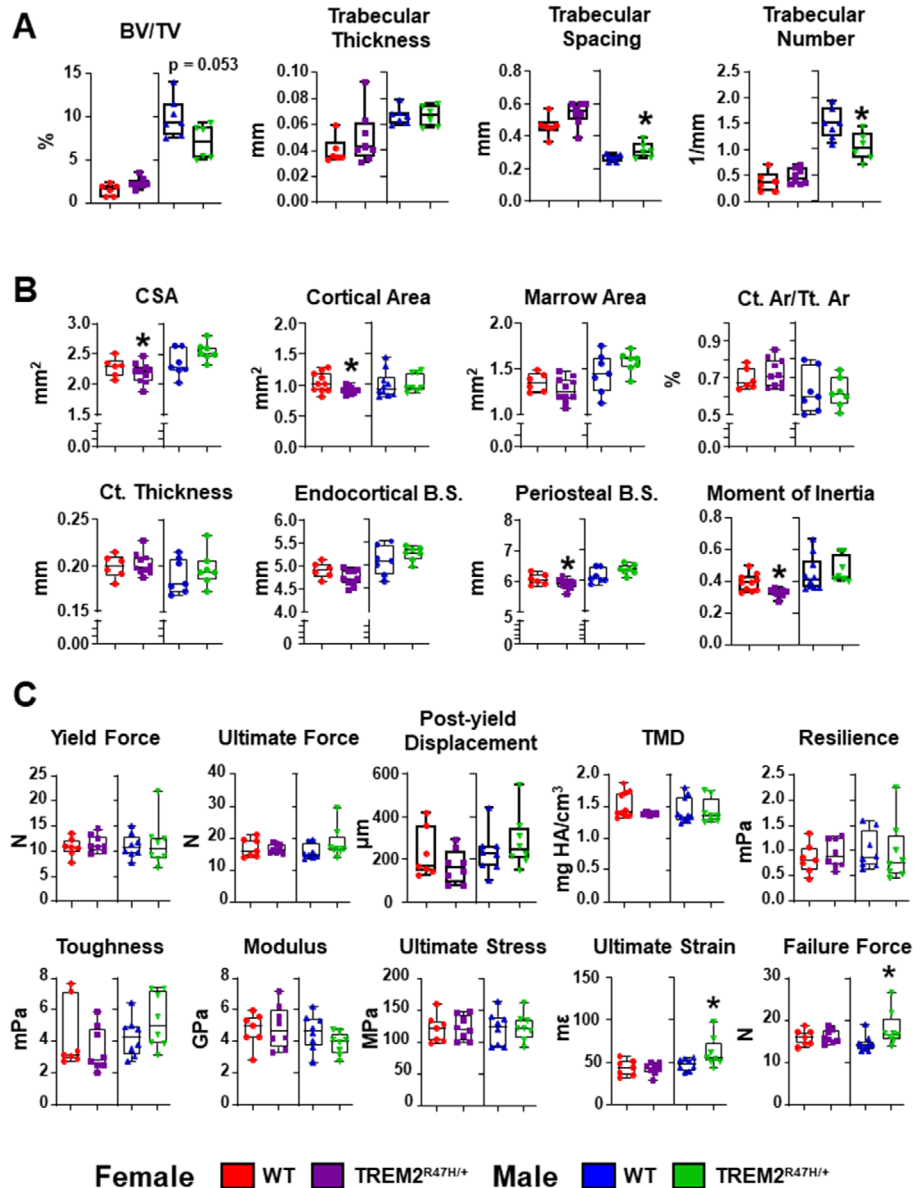


Fig. 3. Age-induced bone loss in male and female $TREM2^{R47H/+}$ animals at 20 months of age. μ CT analysis of cancellous bone of the femoral mid-diaphysis ($n = 5-8$ /group) (A), cortical bone of the distal femur ($n = 6-10$ /group) (B), and three-point bending mechanical testing ($n = 7-10$ /group) (C) in 20-month-old male and female $TREM2^{R47H/+}$ and WT mice. Comparisons are sex-matched, $TREM2^{R47H/+}$ versus WT using Student's *t* test: (A) Male BV/TV $p = 0.0513$, Male trabecular separation $p = 0.047$, Male trabecular number $p = 0.016$. (B) Female cortical area $p = 0.03$, Female periosteal BS $p = 0.011$, Female moment of inertia $p = 0.005$. Comparisons are sex-matched, $TREM2^{R47H/+}$ versus WT using Welch's *t* test: (C) Female TMD $p = 0.055$. Comparisons are sex-matched, $TREM2^{R47H/+}$ versus WT using one-tailed, equal variance *t* test: (A) Female total CSA $p = 0.032$, Female cortical thickness $p = 0.037$. Comparisons are sex-matched, $TREM2^{R47H/+}$ versus WT using Mann-Whitney test: Male failure force $p = 0.015$. Comparisons are sex-matched, $TREM2^{R47H/+}$ versus WT using Welch's one-tailed *t* test: Male ultimate strain $p = 0.039$. TMD = tissue mineral density.

or eroded surface on the femoral endocortical surface, as measured by histomorphometry (Fig. S2A). Dynamic histomorphometry of the femoral mid-diaphysis showed no significant difference in any of the periosteal parameters scored, but there was a slight increase in the endocortical mineral apposition rate of female $TREM2^{R47H/+}$ mice compared to WT mice (Fig. S2B).

Therefore, we decided to further investigate the effect of the $TREM2$ R47H mutation on osteoclasts.

To better understand the effect of the $TREM2$ R47H variant on osteoclast ability to differentiate, non-adherent bone marrow cells isolated from 4-month-old $TREM2^{R47H/+}$ long bones were exposed to RANKL/M-CSF for 2, 5, and 7 days (D2, D5,

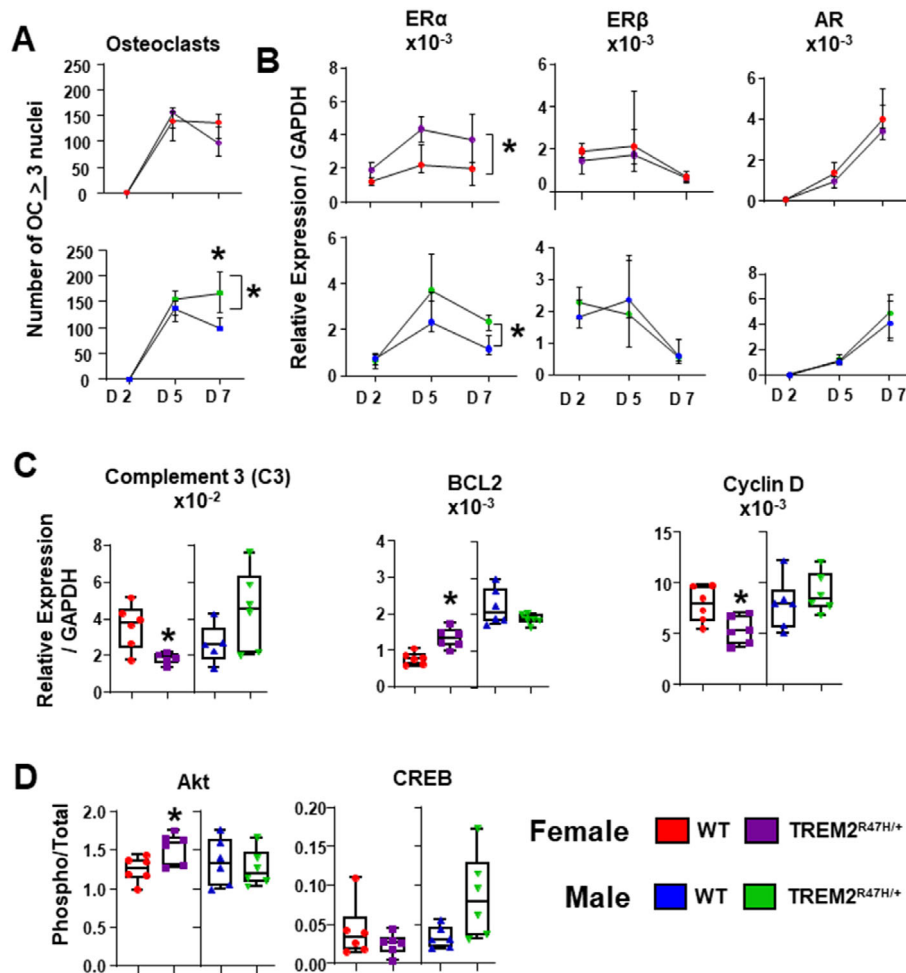


Fig. 4. Sex-dependent alterations in intracellular signaling in TREM2^{R47H/+} osteoclasts. Osteoclast differentiation from male and female, TREM2^{R47H/+} and WT nonadherent bone marrow cells. Cells were differentiated for 2, 5, and 7 days, and the number of TRAP⁺, ≥ 3 nuclei was assessed ($n = 4/5$ wells counted/group) (A), mRNA levels of ER α , ER β , and AR normalized to GAPDH in male and female TREM2^{R47H/+} and WT osteoclasts ($n = 5-6$ /group) (B), mRNA levels of C3, BCL2, and Cyclin D normalized to GAPDH from male and female TREM2^{R47H/+} and WT osteoclasts after 7 days of differentiation ($n = 5-6$ /group) (C), protein multiplex of bone lysates from male and female TREM2^{R47H/+} osteoclasts after 7 days of differentiation (D). Comparisons are sex-matched, TREM2^{R47H/+} versus WT using two-way ANOVA with mixed effects and Sidak's multiple comparisons test: (A) Male TREM2^{R47H/+} versus WT multiple comparison test at D7 $p = 0.0017$. (B) Female ER α expression at D5 $p = 0.024$, D7 $p = 0.018$, Male ER α expression at D5 $p = 0.004$. Comparisons are sex-matched, TREM2^{R47H/+} versus WT using Student's t test: (C) BCL2 $p = 0.0015$, Cyclin D $p = 0.02$. (D) Female Akt $p = 0.0227$. Comparisons are sex-matched, TREM2^{R47H/+} versus WT using Welch's t test: (C) C3 $p = 0.016$. (D) Male CREB $p = 0.0627$. See Table S1 for details on the ANOVA analysis. AR = androgen receptor; C3 = Complement 3; ER α = estrogen receptor alpha; ER β = estrogen receptor beta.

D7), and number of TRAP⁺ osteoclasts with three or more nuclei was quantified. More osteoclasts differentiated from male TREM2^{R47H/+} cells after 7 days of differentiation compared to WT, whereas no difference was found in the number of female TREM2^{R47H/+} osteoclasts (Fig. 4A). However, follow-up gene expression analysis demonstrated that both female and male TREM2^{R47H/+} osteoclasts express significantly higher levels of estrogen receptor α (ER α) mRNA compared to WT cells (Fig. 4B), whereas neither male nor female TREM2^{R47H/+} cells expressed different levels of the sex hormone receptors ER β or androgen receptor (Fig. 4B). To assess whether increased ER α expression might also increase the expression of ER α target genes, we evaluated gene expression of ER α target gene complement 3 (C3) and found that female TREM2^{R47H/+} osteoclasts

had decreased mRNA levels of C3 expression (Fig. 4C). Female TREM2^{R47H/+} osteoclasts also had increased mRNA levels of pro-survival gene BCL2, which suggests the pro-apoptotic effect of estrogen on osteoclasts may be negatively affected by TREM2 R47H expression in female cells (Fig. 4C).

Previous studies have also demonstrated a potential interaction of β -catenin in TREM2 signaling.⁽²⁵⁾ Female TREM2^{R47H/+} osteoclasts express decreased mRNA levels of Wnt/ β -catenin target gene cyclin D1 compared to WT, suggesting the TREM2 R47H mutation may also interact with β -catenin (Fig. 4C). No differences in C3, BCL2, or Cyclin D1 were detected in male TREM2^{R47H/+} osteoclasts compared to WT (Fig. 4C). Together, these data suggest that female TREM2^{R47H/+} osteoclasts exhibit decreased sensitivity to estrogen signaling.

In addition to inducing changes in gene expression, activation of the estrogen receptors can lead to kinase activation, the so-called non-genotropic effects of the receptor.⁽⁵⁵⁾ To test the possibility that the TREM2 R47H variant would affect intracellular kinase activation, multiplex analysis of protein lysates was performed. We found increased phosphorylated protein kinase B (Akt) in female, but not male TREM2^{R47H/+} osteoclasts compared to WT cells (Fig. 4D). However, male but not female TREM2^{R47H/+} osteoclasts had a trend toward increased protein levels of phosphorylated cyclic adenosine monophosphate (cAMP) response element-binding protein (CREB) compared to WT cells (Fig. 4D). Taken together, these data suggest that TREM2^{R47H/+} mutation alters intracellular osteoclast signaling in a sex-dimorphic manner, but only male TREM2^{R47H/+} osteoclast precursors have a cell-autonomous increase in differentiation.

Only female TREM2^{R47H/+} mice have altered body composition and strength

Beyond bone fragility, reduced skeletal muscle strength also significantly contributes to increased risk for falls and fracture that limit mobility and negatively impact patient quality of life.⁽⁵⁶⁾ Skeletal muscle mass and size has been shown to decline with AD progression.⁽⁹⁾ However, no mechanisms for this loss of skeletal muscle mass and strength have been explored. Therefore, we also assessed the skeletal muscle phenotype of female and male TREM2^{R47H/+} mice. Female TREM2^{R47H/+} animals gain body weight differently across 20 months of age, as evaluated by repeated-measures two-way ANOVA (Fig. 5A). This difference seems to be driven by decreases in fat mass percentage and lack of fat mass accrual in female TREM2^{R47H/+} animals, which is not seen in male animals (Fig. 5B). However, there are only mild increases in lean mass percentage in female TREM2^{R47H/+} animals at 6 months of age, but no differences in lean mass between male TREM2^{R47H/+} animals compared to WT (Fig. 5C). Surprisingly, grip strength was significantly increased in female TREM2^{R47H/+} animals at 8 months of age and changed differently compared to WT across 20 months of age, whereas male TREM2^{R47H/+} animals had an increased grip strength only at 8 months of age (Fig. 5D). Activity monitoring of 12-month-old mice showed that female TREM2^{R47H/+} animals spent more time ambulatory, walking around, and less time performing stereotypic movements such as face touching compared to WT littermates, with no differences detected in males (Fig. S3). Lean mass and strength were altered in female but not male TREM2^{R47H/+} animals with age, and this may be explained by these increases in activity.

Muscle-specific changes in strength in female TREM2^{R47H/+} mice

To further assess whether the TREM2 R47H variant alters skeletal muscle strength in a sex-dependent manner, *in vivo* plantarflexion assessment was performed on anesthetized 12-month-old female and male animals. Female TREM2^{R47H/+} mice had increased force across 60 to 150 Hz of stimulation, as well as increased maximal twitch force and force produced at 100 Hz compared to WT littermates, whereas no effect was seen in force production in males (Fig. 6A). Compound muscle action potential (CMAP) stimulation of the sciatic nerve in the same animals demonstrated no differences in sciatic nerve action potential (Fig. S4A, Table S4). These data suggest that the changes in skeletal muscle strength are not likely due to changes in peripheral

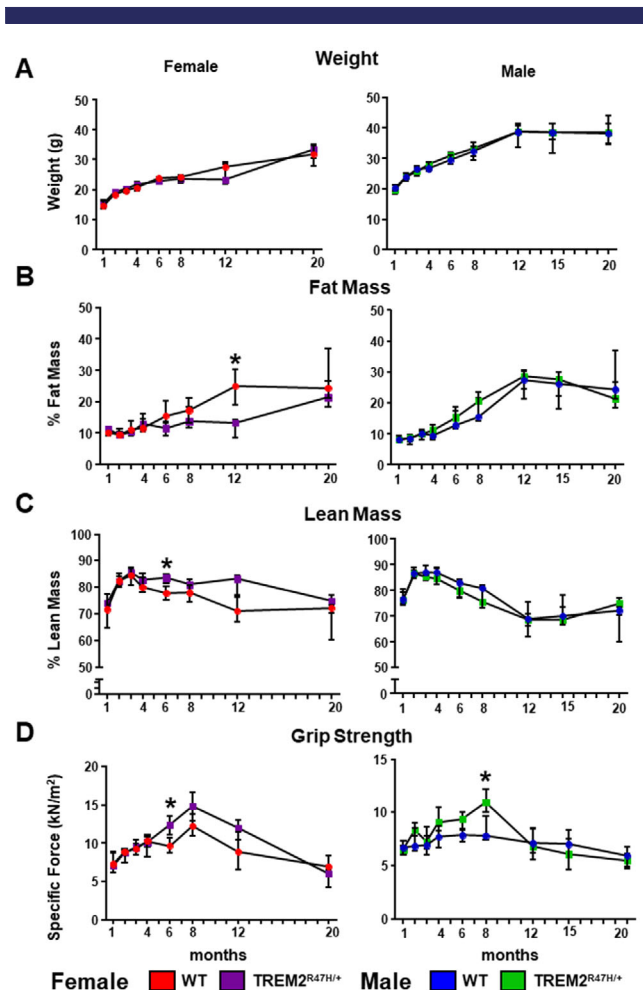


Fig. 5. Body composition and strength are altered in female, but not male TREM2^{R47H/+} animals. Body weight (A), fat mass percentage (B), lean mass percentage (C), and grip strength (D) of male and female TREM2^{R47H/+} animals compared to WT. *n* = 5–8/group. Comparisons are sex- and time-matched, TREM2^{R47H/+} versus WT via RM two-way ANOVA mixed-effect model with Sidak's multiple comparisons test: (B) Female fat mass at 12 months *p* = 0.0085. (C) Female lean mass at 6 months *p* = 0.0319. (D) Female grip strength at 6 months *p* = 0.0027, Male grip strength at 8 months *p* = 0.0023. See Table S2 for details on the ANOVA analysis. RM = repeated measure.

nerve excitability and nervous input to the skeletal muscle. *Ex vivo* skeletal muscle testing of the soleus muscle at the beginning of the fatigue assay showed increases in the twitch force of soleus muscles isolated from 13-month-old female TREM2^{R47H/+} animals compared to WT, but these muscles were also more fatigable as demonstrated by decreases in fatigue percentage (Fig. 6B). Across 40 to 150 Hz of stimulation the 13-month female TREM2^{R47H/+} soleus muscle produced more force than WT (Fig. 6C). However, *ex vivo* testing of the EDL showed no differences in force production or fatigue (Fig. S4B). The soleus is primarily comprised of oxidative Type 1 fibers whereas the EDL is primarily comprised of Type 2B glycolytic fibers, suggesting that the effect of the TREM2 R47H variant on muscle strength but not total lean body mass percentage is due to sex-dependent, fiber-type-specific changes.⁽⁵⁷⁾

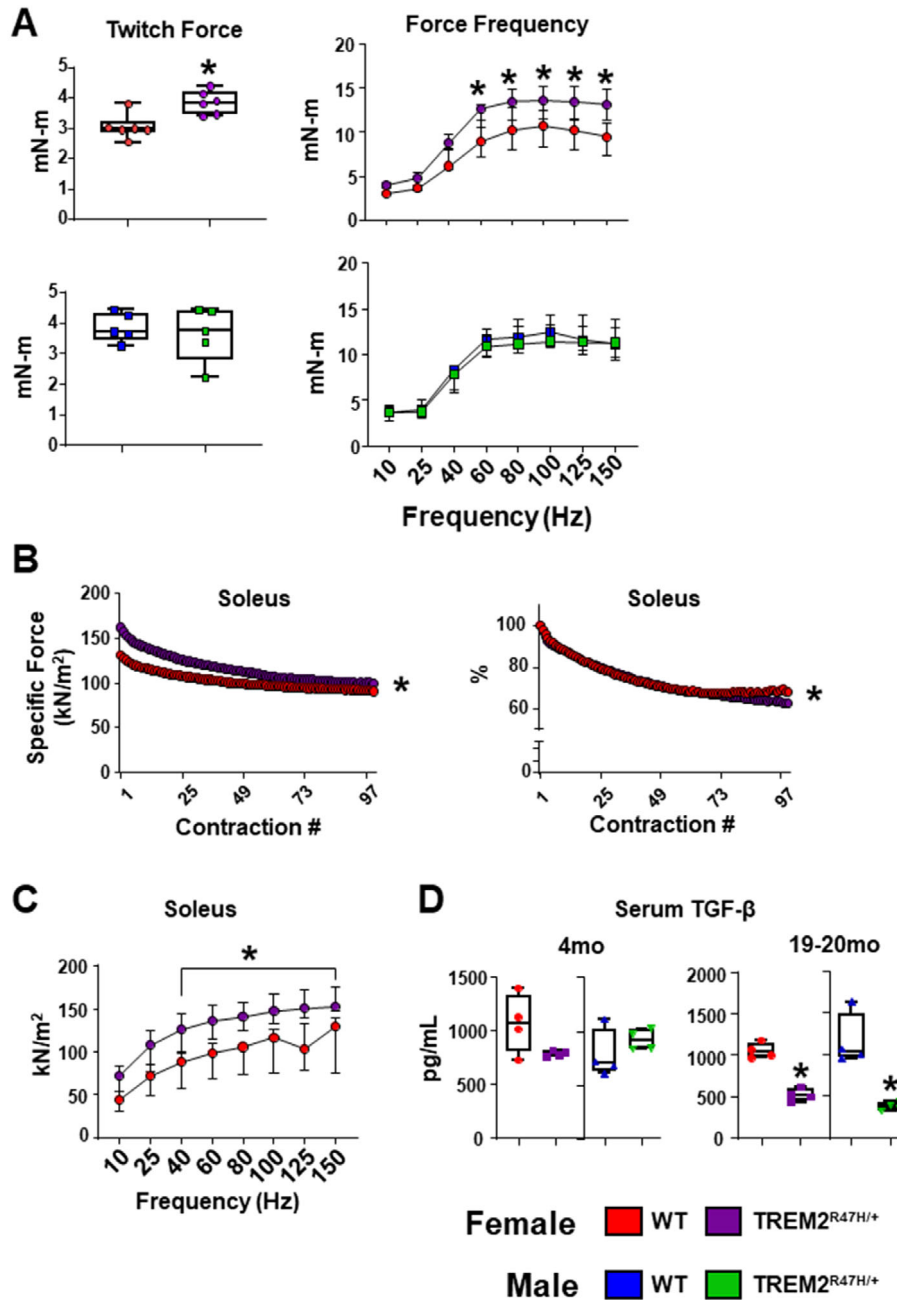


Fig. 6. Increased in vivo plantar flexion and ex vivo soleus contractility muscle strength in female TREM2^{R47H/+} animals at 12 months of age. In vivo plantar flexion of 12-month-old male and female TREM2^{R47H/+} and WT animals demonstrating both maximal twitch force and force production across 150 Hz of stimulation ($n = 5-6$) (A), ex vivo contractility assessment of force production and fatigue of female TREM2^{R47H/+} and WT soleus muscles across 97 contractions ($n = 5-6$ /group) (B), as well as force frequency and force at 100 Hz of stimulation ($n = 5-6$ /group) (C), serum TGF- β levels from 4-month-old and 19-20-month-old male and female TREM2^{R47H/+} and WT animals (D). Force frequency comparison of female TREM2^{R47H/+} to WT using two-way ANOVA and Bonferroni's multiple comparisons: (A) 60 Hz $p = 0.024$, 80 Hz $p = 0.023$, 100 Hz $p = 0.016$, 125 Hz $p = 0.0029$, 150 Hz $p = 0.0006$. (C) 40 Hz $p = 0.0127$, 60 Hz $p = 0.0081$, 80 Hz $p = 0.0031$, 100 Hz $p = 0.0048$, 125 Hz $p = 0.0027$, 150 Hz $p = 0.0029$. Sex-matched comparisons of female and male TREM2^{R47H/+} to WT using Student's t test: (A) Female twitch force $p = 0.0057$. (C) Force at 150 Hz $p = 0.0171$. (D) Female TGF- β 19-20 months $p = 0.0001$. Sex-matched comparisons of male TREM2^{R47H/+} to WT using Mann-Whitney test: Male TGF- β 19-20 months $p = 0.0286$. See Table S3 for details on the ANOVA analysis.

Previous work has demonstrated the importance of bone-muscle crosstalk in disease states, including cancer and burn injury, and with exercise; therefore, we assessed whether the bone-muscle crosstalk mediator transforming growth factor β

(TGF- β) known to be released from the bone matrix during osteoclastic resorption,^(58,59) could be involved in this phenotype. Unexpectedly, however, serum levels of TGF- β are decreased in both female and male TREM2^{R47H/+} animals aged to 19 to 20

months, but not at 4 months (Fig. 6D). Further, C2C12 myotubes after 3 days of differentiation exposed to 10% CM for 48 hours from male (but not female) $TREM2^{R47H/+}$ marrow-flushed long bones were slightly smaller in the average diameter, but frequency distributions demonstrate no differences in the distribution of myotube diameters exposed to either male or female $TREM2^{R47H/+}$ compared to WT bone CM (Fig. S5). These data suggest that the changes in skeletal muscle phenotype seen in $TREM2^{R47H/+}$ animals are likely not associated with alterations of the bone-muscle crosstalk and may be due to other mechanisms.

Discussion

AD is the most common form of dementia worldwide, and disease prevalence is projected to grow over the next 30 years.⁽⁶⁰⁾ AD is most prominently known for impacting memory, but AD patients also exhibit decreases in BMD and skeletal muscle function.^(6,9,61,62) Thus, the impact of AD goes beyond the brain. Nevertheless, there is limited understanding of the mechanisms that contribute to bone fragility and muscle weakness in AD patients. Preclinical studies using mouse models of AD have not conclusively demonstrated that bone fragility and skeletal muscle weakness seen clinically can be explained by the central neurodegeneration of the brain. Neuroinflammation and myeloid cells of the brain have been shown to contribute to AD pathogenesis, and many of these pathways and mechanisms are also present in cells of the bone and skeletal muscle. But whether these mechanisms also contribute to the bone and muscle loss seen clinically independent of the pathology in the brain has been unexplored.

This study focused on the musculoskeletal abnormalities associated with a $TREM2$ variant, known to contribute to neuroinflammation and central pathology in AD via functional changes in microglia, myeloid cells of the brain.⁽⁶³⁾ Previous studies of Nasu-Hakola disease, which is a neurodegenerative disease that also presents with bone cysts, have demonstrated that amino acid substitutions in the $TREM2$ receptor can cause brain and bone disease simultaneously.⁽⁶⁴⁾ However, no AD-associated mutations in $TREM2$ known to contribute to central neurodegeneration have been shown to influence bone or muscle. $TREM2$ expression inhibits osteoclast differentiation and resorption,⁽⁶⁵⁾ but it remains unclear whether amino acid variants known to alter $TREM2$ signaling associated with AD may also alter osteoclast function. Further, there is no existing literature on the role of $TREM2$ in skeletal muscle aging.

In the present study, we used a mouse model of a genetic risk factor for AD carrying the $TREM2$ R47H variant, which lacks the ability to develop central neurodegeneration in the absence of additional mutations, as shown in previous work.^(34,35,66) Our data using this model of AD risk factor has identified a potential mechanism by which bone loss, but not muscle loss, may be explained in AD patients preceding neurodegeneration diagnosis. Global hemizygous expression of the R47H variant used in this study mimics what is seen clinically and allows to better translate the potential effect size of the $TREM2$ R47H variant on bone and muscle. Our data demonstrates this variant only causes bone loss after 13 and 20 months of age in female and male animals, respectively, with a minimum effect in females at 4 months, suggesting the effect of the variant on bone volume is age-dependent and is not involved in skeletal development or maturation.

Late-onset Alzheimer's disease (LOAD), with which the $TREM2$ R47H variant is associated, is typically found in patients ≥ 65 years of age.⁽²⁸⁾ This suggests that age-related changes (eg, cellular senescence/senescence-associated secreted proteins, increased inflammation) that may contribute to $TREM2$ -mediated risk for AD in the brain may also be active in contributing to bone loss and fragility.

Our study identified a poignant sex-dependent effect of the $TREM2$ R47H variant on both bone and muscle. Clinical evidence demonstrates that AD is more prevalent in female compared to male sex, but the mechanism remains unclear. BMD and body composition analysis only showed differences in female, not male, $TREM2^{R47H/+}$ animals across 20 months of age, which prompted us to further investigate the female phenotype by assessing an intermediate time point. Although male animals experience cancellous bone loss and mechanical strength changes at 20 months of age, female animals had much more pronounced changes in bone volume and strength at 13 months of age, and milder differences in cortical bone volume at 20 months of age with no effect on strength. Cortical bone loss was most rapid in the $TREM2^{R47H/+}$ animals between 4 and 13 months of age, where the marrow cavity was larger, the cortical bone was thinner, but the cross-sectional area was larger. Between 13 and 20 months, the female $TREM2^{R47H/+}$ cross-sectional area and periosteal surface become smaller compared to WT. These patterns suggest that age-related periosteal expansion/endocortical resorption in the cortical bone are happening between 4 and 13 months of age in the female $TREM2^{R47H/+}$ animals. Then between 13 and 20 months of age, these patterns stall out and WT animals catch up to conclude with a similar level of bone loss at 20 months of age. These differential rates of bone loss between $TREM2^{R47H/+}$ and WT female mice may explain the lack of difference in the mechanical properties between female $TREM2^{R47H/+}$ and WT femurs at 20 months of age. However, although male $TREM2^{R47H/+}$ animals did not have differences in cortical bone volume at 4 and 20 months of age, there were mild increases in ultimate stress and failure force as measured by three-point bending only at 20 months of age. The only bone loss found in male $TREM2^{R47H/+}$ animals was in the cancellous bone of the distal femur, which was only seen at 20 months of age. This suggests that changes in $TREM2$ signaling in male cells may not impact bone as strongly compared to the females, and may explain why, although $ER\alpha$ mRNA levels and phospho-CREB protein levels were increased in male $TREM2^{R47H/+}$ osteoclasts, there was no effect on bone volume.

The decreased cortical bone volume likely contributes to the decreased mechanical properties seen at 13 months of age in the female $TREM2^{R47H/+}$ animals, although the changes in the material properties and a decrease in the endocortical mineral apposition rate suggest the effect of the $TREM2^{R47H/+}$ variant may go beyond the cell-intrinsic effect of the mutation on osteoclasts and may also impact osteoblast/osteocyte function. This has been described in a clinical case study of Nasu-Hakola disease where a male patient had a mutation in $TREM2$ with abnormal mineralization patterns in the trabecular bone.⁽³²⁾ Interestingly, this case study sample also had a higher BMD in the trabecular bone. Although the mutation in $TREM2$ found in this case study is different from the R47H model reported here, our findings suggest alterations to $TREM2$ signaling may impact osteoblasts. On the other hand, previous work in $TREM2/DAP12$ signaling in osteoclasts has demonstrated that a total loss of $TREM2$ signaling causes increases in osteoclasts as measured by histomorphometry, but no changes in osteoblasts in mice.⁽²⁵⁾

These data suggest that the changes to intracellular cell signaling as a result of variants in TREM2 may alter the paracrine signaling environment impacting osteoblasts. Osteoblasts are not known to express TREM2, hence osteoclast–osteoblast paracrine interactions may mediate effects on bone material properties and dynamic histomorphometry observed in our data. Furthermore, whether TREM2 and the R47H variant also play a role in osteocytes remains unknown. RNA sequencing (RNAseq) data shows TREM2 is expressed, albeit at low levels, in osteocytes and in the osteocytic cell line IDG-SW3, suggesting there may be some cell-intrinsic effects of the TREM2 R47H mutation in this cell type,⁽⁶⁷⁾ although no evidence of TREM2 protein being present in osteocytes has been reported. Therefore, we cannot rule out the possibility that part of the TREM2^{R47H/+} mice phenotype is due to direct consequences of the expression of the variant in osteocytes. Future studies will address the contribution of these cells to the phenotype of mice expressing the TREM2 variant.

In an attempt to find the mediator between osteoclasts and skeletal muscle, we measured the circulating levels of TGF- β , a growth factor known to be deposited in bone by osteoblastic cells and released by osteoclasts following bone resorption. However, osteocytes, which are a differentiated osteoblast embedded in the bone and create an interconnected network, are also known to be significantly impacted by TGF- β . Previous work has shown that the osteocyte network and bone volume are negatively impacted in a sex-dependent manner by loss of TGF- β signaling using a T β 2R^{-/-} mouse model; however, an effect was seen in male and not female animals, suggesting that either a different receptor is involved or that other mechanisms are contributing to our observed phenotype beyond loss of TGF- β signaling.⁽⁶⁸⁾ Other work has also defined a role for TGF- β signaling in bone material strength, suggesting the potential involvement of osteocytes on the effects of the growth factor.⁽⁶⁹⁾ Yet whether this effect is sex dimorphic or consistent with the data presented herein remains unclear. Further, we show herein an age-related decreases in circulating TGF- β levels, but osteocyte scoring shows no difference in the number of osteocytes in the cortical compartment of the femur. Therefore, our data does not provide conclusive evidence for or against direct consequences of the TREM2 R47H variant on osteocytes. Rather, future studies will need to define whether TREM2 is expressed in osteocytes at the protein level, if this expression changes with age, if TREM2 interacts with TGF- β in osteocytes, and whether the R47H variant alters osteocyte function directly or indirectly.

The data presented in our study suggest the R47H variant may alter intracellular osteoclast signaling in a sex-dependent manner. In female animals, the R47H variant seems to modify the interaction of TREM2 signaling with ER α -mediated estrogen signaling via Akt. Changes in cyclin D1 also indicate the R47H variant may alter Wnt/ β -catenin signaling, which is consistent with previous studies in TREM2 knockout models.⁽²⁵⁾ AD is thought to be more common in females compared to males, which suggests that sex-dependent prevalence of AD may be explained by changes in ER α signaling. Consistent with previous reports in macrophages that cell differentiation and activity is only mildly impacted by the R47H mutation, osteoclast differentiation was mildly increased only in male osteoclasts.⁽³⁰⁾ Future work will be needed to directly evaluate whether osteoclast activity is also sex-dependent. However, why increased AD prevalence in women is dependent on geographic location or other sex-dependent risk factors remains uncertain.^(70,71) In a mouse model of APOE4 expression, another strong genetic risk factor for AD, TREM2 expression and microglial response to plaque in

the brain was also different between female and male animals.⁽⁷²⁾ Although these data were generated in microglia of the brain, they suggest that TREM2 signaling may contribute to sex-dependent differences in risk and pathology of AD, and our data suggest that this may be true in multiple tissues including bone and muscle.

Lean mass and muscle strength have been shown to be decreased in AD patients, but whether this impairment is regulated in a sex-dependent manner remains unclear.^(9,10,61) Our data shows that female TREM2^{R47H/+} animals weighed less than WT, and this was driven primarily by decreases in fat mass which likely had some degree of influence on the mild increase in lean mass. Surprisingly, female TREM2^{R47H/+} animals are also stronger, but these changes in body composition and strength is not likely influenced by changes in activity levels, suggesting other mechanisms may be at play. TGF- β is known to be secreted from the bone matrix via resorption and has been shown to cause skeletal muscle atrophy in mouse models of high osteoclastic resorption.^(59,73) Because our female and male animals experience bone loss by 20 months of age, we investigated whether TGF- β could play a role in these observed changes in body composition. Interestingly, although significant decreases in TGF- β in the circulation were seen in both female and male animals, strength changes were only observed in female animals. Thus, the mechanism leading to increased muscle strength in female TREM2^{R47H/+} mice may be related to the decreased pro-atrophic signals resulting from lower TGF- β levels, though this does not explain the lack of effect on male animals, therefore suggesting that additional unknown mechanisms may be involved.

Ex vivo muscle contractility measurement demonstrated increases in the soleus strength, not the EDL, suggesting that the change in strength may also be muscle specific. Aging skeletal muscle is known to undergo fiber-type-specific changes, primarily affecting glycolytic, Type II fibers which are the predominant fiber type found in the EDL.^(74,75) These Type II fibers that make up the majority of the EDL have been shown to express more Activin receptor type-2B (ACVR1B) receptors for TGF- β and its family members, including activin, myostatin, and growth differentiation factor 11 (GDF11), than the Type I fibers that make up a majority of the soleus, making it unlikely that the decreased TGF- β had a strong effect on the soleus strength but not the EDL.⁽⁷⁶⁾

Our mRNA expression data demonstrate skeletal muscle fibers do not express TREM2, and our bone conditioned media experiment suggests bone–muscle crosstalk cannot likely explain our observed changes in skeletal muscle of female TREM2^{R47H/+} mice. Thus, another cell type in skeletal muscle may be involved in this observed phenotype. Macrophages, known to express TREM2, exist in the skeletal muscle as intramuscular macrophages. These macrophages are known to play a role in skeletal muscle regeneration and repair after injury and exercise, but also are thought to be involved in age-related skeletal muscle weakness.⁽⁷⁷⁾ No data has ever described a role for TREM2 in skeletal muscle during aging, although changes in intramuscular macrophage cell population are known to contribute to age-related skeletal muscle weakness. Previous work has demonstrated an increased ratio of M2/M1 macrophages in aged versus young skeletal muscle, and that these macrophages associate with intramuscular adipose tissue.⁽⁷⁸⁾ Further, it is known that the soleus muscle has a higher proportion of intramuscular macrophages compared to the gastrocnemius.⁽⁷⁹⁾ Therefore, it is possible that intramuscular macrophage function altered due to the

TREM2 R47H variant may explain the fiber type-specific changes in skeletal muscle strength. Here we used a model of global expression of the R47H variant, hence our study does not allow us to explicitly identify intramuscular macrophages as the cause of the phenotype, although we cannot exclude macrophages from consideration as contributors to the phenotype. Therefore, more work is needed to clearly define the role of the intramuscular macrophage in muscle weakness and sarcopenia, and future studies will be needed to address how TREM2 expression, and the R47H variant, in these intramuscular macrophages may impact skeletal muscle mass and strength with age.

Overall, this study suggests that mechanisms active in perpetuating AD pathogenesis in the brain may also be active in other tissues that are known to be negatively affected by AD. These data demonstrate that genetic risk factors known to contribute to the pathology of AD in the brain can also cause transient bone loss and fragility, but not muscle weakness, independent of pathology in the brain in female but not male animals. Further work will be needed to assess when in the aging process these mechanisms become detrimental to bone volume and fragility, and what triggers this degeneration. Additionally, although our data implicates a role of TREM2 in skeletal muscle strength, more work is needed to identify what cell types expressing TREM2 may contribute to skeletal muscle strength regulation, and the mechanism for this interaction. In this study, A β plaques, or tau neurofibrillary tangles were not present, suggesting that other age-related changes may be triggering TREM2-dependent degenerative mechanisms in tissues beyond the brain.

Acknowledgments

Studies were funded by the Veterans Research Administration Merit Award 110 1BX005154 to LIP, the American Cancer Society Research Scholar Grant 132013-RSG-18-010-01-CCG, the National Institute of Arthritis and Musculoskeletal and Skin Diseases R01AR079379 and a IUPUI Research Support Funds Grant to AB, and an Indiana Center for Musculoskeletal Health multi-PI pilot project award to LIP and AB. ALE and JRH were supported by a NIH-NIAMS T32-AR065971 - Comprehensive Musculoskeletal Training Program (T32), Indiana University School of Medicine (IUSM), Indianapolis, IN. ALE was also supported in part by funds from the Department of Otolaryngology-Head & Neck Surgery to AB. We thank Dr. Ziyue Liu for help with the statistics methods used in this study.

Author Contributions

Alyson Essex: Conceptualization; formal analysis; investigation; methodology; writing – original draft; writing – review and editing. **Joshua R Huot:** Formal analysis; methodology; writing – review and editing. **Padmini Deosthale:** Formal analysis; investigation; writing – review and editing. **Allison Wagner:** Formal analysis; writing – review and editing. **Jorge Figueras:** Formal analysis; writing – review and editing. **Azaria Davis:** Formal analysis; writing – review and editing. **John G Damrath:** Formal analysis; methodology; writing – review and editing. **Fabrizio Pin:** Formal analysis; writing – review and editing. **Joseph M Wallace:** Methodology; software; writing – review and editing. **Andrea Bonetto:** Conceptualization; funding acquisition; methodology; resources; supervision; writing – review and editing. **Lilian Plotkin:** Conceptualization; funding acquisition; methodology;

project administration; supervision; writing – original draft; writing – review and editing.

Peer Review

The peer review history for this article is available at <https://publons.com/publon/10.1002/jbmr.4572>.

Data Availability Statement

The data that support the findings of this study are available from the corresponding author upon reasonable request.

References

- 2021 Alzheimer's disease facts and figures. *Alzheimers Dement.* 2021;17(3):327-406.
- Briggs AM, Cross MJ, Hoy DG, et al. Musculoskeletal health conditions represent a global threat to healthy aging: a report for the 2015 World Health Organization world report on ageing and health. *Gerontologist.* 2016;56(Suppl 2):S243-S255.
- Harvey N, Dennison E, Cooper C. Osteoporosis: impact on health and economics. *Nat Rev Rheumatol.* 2010;6(2):99-105.
- DeTure MA, Dickson DW. The neuropathological diagnosis of Alzheimer's disease. *Mol Neurodegener.* 2019;14(1):32.
- Bliuc D, Tran T, Adachi JD, et al. Cognitive decline is associated with an accelerated rate of bone loss and increased fracture risk in women: a prospective study from the Canadian Multicentre Osteoporosis Study. *J Bone Miner Res.* 2021;36(11):2106-2115.
- Loskutova N, Honea RA, Vidoni ED, Brooks WM, Burns JM. Bone density and brain atrophy in early Alzheimer's disease. *J Alzheimers Dis.* 2009;18(4):777-785.
- Loskutova N, Watts AS, Burns JM. The cause-effect relationship between bone loss and Alzheimer's disease using statistical modeling. *Med Hypotheses.* 2019;122:92-97.
- Tan ZS, Seshadri S, Beiser A, et al. Bone mineral density and the risk of Alzheimer disease. *Arch Neurol.* 2005;62(1):107-101.
- Ogawa Y, Kaneko Y, Sato T, Shimizu S, Kanetaka H, Hanyu H. Sarcopenia and muscle functions at various stages of Alzheimer disease. *Front Neurol.* 2018;9:710.
- Burns JM, Johnson DK, Watts A, Swerdlow RH, Brooks WM. Reduced lean mass in early Alzheimer disease and its association with brain atrophy. *Arch Neurol.* 2010;67(4):428-233.
- Cui S, Xiong F, Hong Y, et al. APPswe/A β regulation of osteoclast activation and RAGE expression in an age-dependent manner. *J Bone Miner Res.* 2011;26(5):1084-1098.
- Yang M-W, Wang T-H, Yan P-P, et al. Curcumin improves bone micro-architecture and enhances mineral density in APP/PS1 transgenic mice. *Phytomedicine.* 2011;18(2):205-213.
- Radde R, Bolmont T, Kaeser SA, et al. Abeta42-driven cerebral amyloidosis in transgenic mice reveals early and robust pathology. *EMBO Rep.* 2006;7(9):940-946.
- Tinetti ME, Speechley M, Ginter SF. Risk factors for falls among elderly persons living in the community. *N Engl J Med.* 1988;319(26):1701-1707.
- Dev K, Javed A, Bai P, et al. Prevalence of falls and fractures in Alzheimer's patients compared to general population. *Cureus.* 2021;13(1):e12923.
- Jay TR, von Saucken VE, Landreth GE. TREM2 in neurodegenerative diseases. *Mol Neurodegener.* 2017;12(1):56.
- Filipello F, Morini R, Corradini I, et al. The microglial innate immune receptor TREM2 is required for synapse elimination and Normal brain connectivity. *Immunity.* 2018;48(5):979-991.e8.
- Gervois P, Lambrichts I. The emerging role of triggering receptor expressed on myeloid cells 2 as a target for immunomodulation in ischemic stroke. *Front Immunol.* 2019;10:1668.

19. Liu W, Taso O, Wang R, et al. Trem2 promotes anti-inflammatory responses in microglia and is suppressed under pro-inflammatory conditions. *Hum Mol Genet.* 2020;29(19):3224-3248.
20. Ulrich JD, Ulland TK, Colonna M, Holtzman DM. Elucidating the role of TREM2 in Alzheimer's disease. *Neuron.* 2017;94(2):237-248.
21. Jay TR, Hirsch AM, Broihier ML, et al. Disease progression-dependent effects of TREM2 deficiency in a mouse model of Alzheimer's disease. *J Neurosci.* 2017;37(3):637-647.
22. Ransohoff RM. How neuroinflammation contributes to neurodegeneration. *Science.* 2016;353(6301):777-783.
23. Wang Y, Ulland TK, Ulrich JD, et al. TREM2-mediated early microglial response limits diffusion and toxicity of amyloid plaques. *J Exp Med.* 2016;213(5):667-675.
24. Yuan P, Condello C, Keene CD, et al. TREM2 haploinsufficiency in mice and humans impairs the microglia barrier function leading to decreased amyloid compaction and severe axonal dystrophy. *Neuron.* 2016;90(4):724-739.
25. Otero K, Shinohara M, Zhao H, et al. TREM2 and β -catenin regulate bone homeostasis by controlling the rate of osteoclastogenesis. *J Immunol.* 2012;188(6):2612-2621.
26. Humphrey MB, Daws MR, Spusta SC, et al. TREM2, a DAP12-associated receptor, regulates osteoclast differentiation and function. *J Bone Miner Res.* 2006;21(2):237-245.
27. Jay TR, Miller CM, Cheng PJ, et al. TREM2 deficiency eliminates TREM2+ inflammatory macrophages and ameliorates pathology in Alzheimer's disease mouse models. *J Exp Med.* 2015;212(3):287-295.
28. Korvatska O, Leverenz JB, Jayadev S, et al. R47H variant of TREM2 associated with Alzheimer disease in a large late-onset family: clinical, genetic, and neuropathological study. *JAMA Neurol.* 2015;72(8):920-927.
29. Cheng-Hathaway PJ, Reed-Geaghan EG, Jay TR, et al. The Trem2 R47H variant confers loss-of-function-like phenotypes in Alzheimer's disease. *Mol Neurodegener.* 2018;13(1):29.
30. Hall-Roberts H, Agarwal D, Obst J, et al. TREM2 Alzheimer's variant R47H causes similar transcriptional dysregulation to knockout, yet only subtle functional phenotypes in human iPSC-derived macrophages. *Alzheimers Res Ther.* 2020;12(1):151.
31. Dean HB, Roberson ED, Song Y. Neurodegenerative disease-associated variants in TREM2 destabilize the apical ligand-binding region of the immunoglobulin domain. *Front Neurol.* 2019;10:1252.
32. Shboul M, Roschger P, Ganger R, et al. Bone matrix hypermineralization associated with low bone turnover in a case of Nasu-Hakola disease. *Bone.* 2019;123:48-55.
33. Guerreiro R, Wojtas A, Bras J, et al. TREM2 variants in Alzheimer's disease. *N Engl J Med.* 2013;368(2):117-127.
34. Kotredes K, Oblak A, Pandey R, et al. A multi-discipline phenotyping platform for late-onset Alzheimer's disease employed on a novel, humanized APOE4.Trem2*R47H mouse model. *Research Gate;* 2020. <https://doi.org/10.21203/rs.3.rs-135213/v1>.
35. Foidl BM, Humpel C. Can mouse models mimic sporadic Alzheimer's disease? *Neural Regen Res.* 2020;15(3):401-406.
36. Pacheco-Costa R, Hassan I, Reginato RD, et al. High bone mass in mice lacking Cx37 due to defective osteoclast differentiation. *J Biol Chem.* 2014;289(12):8508-8520.
37. Pin F, Barreto R, Kitase Y, et al. Growth of ovarian cancer xenografts causes loss of muscle and bone mass: a new model for the study of cancer cachexia. *J Cachexia Sarcopenia Muscle.* 2018;9(4):685-700.
38. Wallace JM, Golcuk K, Morris MD, Kohn DH. Inbred strain-specific effects of exercise in wild type and biglycan deficient mice. *Ann Biomed Eng.* 2010;38(4):1607-1617.
39. Aguilar-Perez A, Pacheco-Costa R, Atkinson EG, et al. Age- and sex-dependent role of osteocytic pannexin1 on bone and muscle mass and strength. *Sci Rep.* 2019;9(1):13903.
40. Jepsen KJ, Silva MJ, Vashishth D, Guo XE, van der Meulen MC. Establishing biomechanical mechanisms in mouse models: practical guidelines for systematically evaluating phenotypic changes in the diaphyses of long bones. *J Bone Miner Res.* 2015;30(6):951-966.
41. Davis HM, Aref MW, Aguilar-Perez A, et al. Cx43 overexpression in osteocytes prevents osteocyte apoptosis and preserves cortical bone quality in aging mice. *JBMR Plus.* 2018;2(4):206-216. <https://doi.org/10.1002/jbmr4.10035>.
42. Dempster DW, Compston JE, Drezner MK, et al. Standardized nomenclature, symbols, and units for bone histomorphometry: a 2012 update of the report of the ASBMR Histomorphometry Nomenclature Committee. *J Bone Miner Res.* 2013;28(1):2-17.
43. Davis HM, Pacheco-Costa R, Atkinson EG, et al. Disruption of the Cx43/miR21 pathway leads to osteocyte apoptosis and increased osteoclastogenesis with aging. *Aging Cell.* 2017;16(3):551-563.
44. Toledo M, Penna F, Oliva F, et al. A multifactorial anti-cachectic approach for cancer cachexia in a rat model undergoing chemotherapy. *J Cachexia Sarcopenia Muscle.* 2016;7(1):48-59.
45. Huot JR, Pin F, Essex AL, Bonetto A. MC38 tumors induce musculoskeletal defects in colorectal cancer. *Int J Mol Sci.* 2021;22(3):1486.
46. Huot JR, Pin F, Narasimhan A, et al. ACVR2B antagonism as a countermeasure to multi-organ perturbations in metastatic colorectal cancer cachexia. *J Cachexia Sarcopenia Muscle.* 2020;11(6):1779-1798.
47. Arnold WD, Sheth KA, Wier CG, Kissel JT, Burghes AH, Kolb SJ. Electrophysiological motor unit number estimation (MUNE) measuring compound muscle action potential (CMAP) in mouse hindlimb muscles. *J Vis Exp.* 2015;(103):e52899.
48. Sheth KA, Iyer CC, Wier CG, et al. Muscle strength and size are associated with motor unit connectivity in aged mice. *Neurobiol Aging.* 2018;67:128-136.
49. Pin F, Novinger LJ, Huot JR, et al. PDK4 drives metabolic alterations and muscle atrophy in cancer cachexia. *FASEB J.* 2019;33(6):7778-7790.
50. Davis HM, Deosthale PJ, Pacheco-Costa R, et al. Osteocytic miR21 deficiency improves bone strength independent of sex despite having sex divergent effects on osteocyte viability and bone turnover. *FEBS J;*2020(287, 5):941-963.
51. Schneider CA, Rasband WS, Eliceiri KW. NIH Image to ImageJ: 25 years of image analysis. *Nat Methods.* 2012;9(7):671-675.
52. Ruxton GD, Neuhäuser M. When should we use one-tailed hypothesis testing? *Methods Ecol Evol.* 2010;1(2):114-114.
53. Ludbrook J. Should we use one-sided or two-sided P values in tests of significance? *Clin Exp Pharmacol Physiol.* 2013;40(6):357-361.
54. Xiang X, Piers TM, Wefers B, et al. The Trem2 R47H Alzheimer's risk variant impairs splicing and reduces Trem2 mRNA and protein in mice but not in humans. *Mol Neurodegener.* 2018;13(1):49.
55. Kousteni S, Han L, Chen JR, et al. Kinase-mediated regulation of common transcription factors accounts for the bone-protective effects of sex steroids. *J Clin Invest.* 2003;111(11):1651-1664.
56. Yeung SSY, Reijnierse EM, Pham VK, et al. Sarcopenia and its association with falls and fractures in older adults: a systematic review and meta-analysis. *J Cachexia Sarcopenia Muscle.* 2019;10(3):485-500.
57. Schiaffino S, Reggiani C. Fiber types in mammalian skeletal muscles. *Physiol Rev.* 2011;91(4):1447-1531.
58. Bonewald L. Use it or lose it to age: a review of bone and muscle communication. *Bone.* 2019;120:212-218.
59. Waning DL, Mohammad KS, Reiken S, et al. Excess TGF-beta mediates muscle weakness associated with bone metastases in mice. *Nat Med.* 2015;21(11):1262-1271.
60. Alzheimer's Association. 2016 Alzheimer's disease facts and figures. *Alzheimers Dement.* 2016;12(4):459-509.
61. Boyle PA, Buchman AS, Wilson RS, Leurgans SE, Bennett DA. Association of muscle strength with the risk of Alzheimer disease and the rate of cognitive decline in community-dwelling older persons. *Arch Neurol.* 2009;66(11):1339-1344.
62. Daulatzai MA. Early stages of pathogenesis in memory impairment during normal senescence and Alzheimer's disease. *J Alzheimers Dis.* 2010;20:355-367.
63. Zhou SL, Tan CC, Hou XH, Cao XP, Tan L, Yu JT. TREM2 variants and neurodegenerative diseases: a systematic review and meta-analysis. *J Alzheimers Dis.* 2019;68(3):1171-1184.
64. Xing J, Titus AR, Humphrey MB. The TREM2-DAP12 signaling pathway in Nasu-Hakola disease: a molecular genetics perspective. *Res Rep Biochem.* 2015;5:89-100.

65. Otero K, Shinohara M, Zhao H, et al. TREM2 and beta-catenin regulate bone homeostasis by controlling the rate of osteoclastogenesis. *J Immunol*. 2012;188(6):2612-2621.
66. Guo Q, Li H, Cole AL, Hur J-Y, Li Y, Zheng H. Modeling Alzheimer's disease in mouse without mutant protein overexpression: cooperative and independent effects of A β and tau. *PLoS One*. 2013;8(11):e80706.
67. Youlten SE, Kemp JP, Logan JG, et al. Osteocyte transcriptome mapping identifies a molecular landscape controlling skeletal homeostasis and susceptibility to skeletal disease. *Nat Commun*. 2021;12(1):2444.
68. Dole NS, Yee CS, Mazur CM, Acevedo C, Alliston T. TGFbeta regulation of perilacunar/canalicular remodeling is sexually dimorphic. *J Bone Miner Res*. 2020;35(8):1549-1561.
69. Dole NS, Mazur CM, Acevedo C, et al. Osteocyte-intrinsic TGF-beta signaling regulates bone quality through perilacunar/canalicular remodeling. *Cell Rep*. 2017;21(9):2585-2596.
70. Zhu D, Montagne A, Zhao Z. Alzheimer's pathogenic mechanisms and underlying sex difference. *Cell Mol Life Sci*. 2021;78(11):4907-4920.
71. Nebel RA, Aggarwal NT, Barnes LL, et al. Understanding the impact of sex and gender in Alzheimer's disease: a call to action. *Alzheimers Dement*. 2018;14(9):1171-1183.
72. Stephen TL, Cacciottolo M, Balu D, et al. APOE genotype and sex affect microglial interactions with plaques in Alzheimer's disease mice. *Acta Neuropathol Commun*. 2019;7(1):82.
73. Regan JN, Trivedi T, Guise TA, Waning DL. The role of TGFbeta in bone-muscle crosstalk. *Curr Osteoporos Rep*. 2017;15(1):18-23.
74. Miljkovic N, Lim JY, Miljkovic I, Frontera WR. Aging of skeletal muscle fibers. *Ann Rehabil Med*. 2015;39(2):155-162.
75. Tarantino U, Baldi J, Celi M, et al. Osteoporosis and sarcopenia: the connections. *Aging Clin Exp Res*. 2013;25(Suppl 1):S93-S95.
76. Mendias CL, Marcin JE, Calerdon DR, Faulkner JA. Contractile properties of EDL and soleus muscles of myostatin-deficient mice. *J Appl Physiol*. 2006;101(3):898-905.
77. Saclier M, Cuvellier S, Magnan M, Mounier R, Chazaud B. Monocyte/macrophage interactions with myogenic precursor cells during skeletal muscle regeneration. *FEBS J*. 2013;280(17):4118-4130.
78. Cui C-Y, Driscoll RK, Piao Y, Chia CW, Gorospe M, Ferrucci L. Skewed macrophage polarization in aging skeletal muscle. *Aging Cell*. 2019;18(6):e13032.
79. Reidy PT, McKenzie AI, Mahmassani ZS, et al. Aging impairs mouse skeletal muscle macrophage polarization and muscle-specific abundance during recovery from disuse. *Am J Physiol Endocrinol Metab*. 2019;317(1):E85-E98.